Interference Signatures of Abelian and Non-Abelian Aharonov-Bohm effect on Neutral Atoms in Optical Lattices

Ming-Xia Huo,[1] Nie Wei,[1] David A.W. Hutchinson,[1,2] and Leong Chuan Kwek[1,3]

[1] *Centre for Quantum Technologies, National University of Singapore, 3 Science Drive 2, Singapore 117543*
[2] *Centre for Quantum Technology, Department of Physics, University of Otago, Dunedin, New Zealand*
[3] *National Institute of Education and Institute of Advanced Studies, Nanyang Technological University, 1 Nanyang Walk, Singapore 637616*

We propose a scheme to generate an effective Abelian U(1) or non-Abelian SU(2) gauge field for cold neutral atoms in a ring- or square-shaped optical lattice by using Laguerre-Gauss lasers. The synthetic field produced is strongly localized allowing us to study the Aharonov-Bohm effect on the neutral atoms. By preparing a coherent state of atoms initially and allowing them to evolve along two different paths enclosing the generated magnetic field, we obtain interference signatures of the Aharonov-Bohm effect with distinctly different patterns in the detection area for systems exposed to a zero, an Abelian U(1) or a non-Abelian SU(2) gauge field.

PACS numbers: 03.75.Lm, 03.75.Mn, 03.75.Kk, 11.15.Ha

The vector potential, introduced by Maxwell and Thomson as a mathematical tool to describe Faraday's field, changed ontologically with the discovery of the Aharonov-Bohm (AB) effect [1]. The AB phase is the archetypical example of a geometric phase as introduced by Berry [2]. As such it has spawn many experimental and theoretical studies and remains of intense interest. Numerous realizations of the AB effect have been studied [3–5]. Furthermore, in condensed matter, several AB-like effects for charged particles have been investigated [6], including graphene nanostructures [7], quantum rings,dots and mesoscopic devices [8, 9], and carbon nanotubes [10].

Ultracold atoms, with their unprecedented control over both internal and external degrees of freedom, in optical lattices offer a further opportunity to investigate these phenomena by utilizing synthetic gauge fields. These synthetic fields can be produced in various ways including rotation of the confining trap [11, 12], using adiabatic motion of multilevel atoms in a dark-state picture [13], employing spatially dependent two-photon dressing [14], and using staggered-aligned states [15] or rotations [16] for lattice gauge theories. Further additional terms such as spin-orbit coupling have also been added to the emulated Hamiltonian [17].

Motivated by these studies, we propose a scheme to generate Abelian and non-Abelian fields, utilizing laser-assisted tunneling [18]. This scheme generates an almost perfect solenoid and hence we can investigate theoretically the AB effect and its non-Abelian analogue in the presence of these fields. In addition, we note that non-Abelian gauge fields have been mooted as possible sources of topological order of relevance in the context of topological insulators [19, 20] and topological quantum computing [21].

Model Setup and Basic Principle: We propose a scheme to employ Laguerre-Gauss (LG) laser beams to assist inter-site tunneling and realize an artificial gauge potential in both a square lattice Fig. 1(a) and in a ring geometry Fig. 1(b) [22]. A natural property of the LG laser is a spatially dependent orbital angular momentum along a closed loop. Our scheme therefore provides an extremely simple alternative way to produce a non-vanishing effective magnetic, or more exotic, gauge field for neutral atoms, without the need for rotation, lattice accelerations, or the stringent external field conditions necessary to utilize degenerate dark states. Apart from the usual square lattice as shown in Fig. 1 (a) which can be created by the interference of counter-propagating laser beams, a ring lattice in (b) can also be created by interfering an off-resonant LG laser and a plane wave $E_0 e^{i(\omega_0 t - k_0 z)}$. In

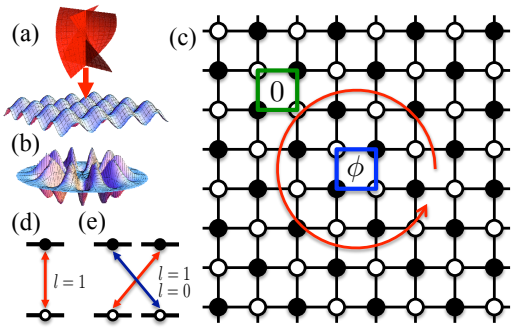

FIG. 1: Schematic diagram for generating effective magnetic fields with cold atoms trapped in square (a) and ring (b) lattices. The atoms can hop from one site to a neighboring site via laser-assisted tunneling by shinning LG lasers perpendicular to the lattice surface (a). The LG beams drive the spin-conserved transitions between two identical sublevels in neighboring sites in (d) to generate Abelian fields, and spin-flipping transitions between two different sublevels in neighboring sites in (e) to generate SU(2) non-Abelian fields. The resulting magnetic flux as shown in (c) is non-zero when going around a loop including the laser center which is addressed in the lattice center and zero when the laser center is excluded from the loop.

cylindrical coordinates, an LG laser mode with frequency ω_0, wave vector k_0, and amplitude E_0 propagating along the z axis can be denoted by

$$E_0 f_{p_0 l_0}(r_0)\, e^{i l_0 \varphi_0} e^{i(\omega_0 t - k_0 z)},$$

where $f_{pl}(r) = (-1)^p \times \sqrt{\frac{2p!}{\pi(p+|l|)!}} \xi^{|l|} L_p^{|l|} \xi^2 e^{-\xi^2}$, $\xi = \frac{\sqrt{2}r}{r_{\rm w}}$, $r_{\rm w}$ is the waist of the beam, and $L_p^{|l|}$ are the Laguerre functions [22]. The labels p and l represent the radial and azimuthal quantum numbers, respectively. The interference of the LG beam and the plane wave produce the periodic interferogram in φ_0 with l_0 wells. After loading atoms into the square lattice in (a) or the 1D ring in (b), we apply Raman LG lasers $E f_{pl}(r)\, e^{il\varphi} e^{i(\omega t - kz)}$ perpendicular to the lattice, as illustrated in (a), to drive atomic hopping from site to site. We note that any laser-assisted tunneling scheme can be used for this step. For example, one can trap atoms in a hyperfine-level-independent superlattice $V(\overrightarrow{r}) = V_0 \sum_a \left[\cos^2(\pi r_a) + \cos^2(2\pi r_a)\right]$ with $V_0 \sim 50 - 150$kHz. Using ^{40}K atoms with hyperfine levels $F = \frac{9}{2}$ as effective spins in the zero-energy main sites and $F = \frac{7}{2}$ as intermediate links with energy around $50 - 100$kHz [23], the coherent LG lasers induce tunneling of spins $F = \frac{9}{2}$ along a ring as shown in Fig. 1(c). Utilizing one Zeeman level in $F = \frac{9}{2}$ generates an Abelian field [figure 1(d)] whilst using two Zeeman levels generates SU(2) non-Abelian field [figure 1(e)]. We can also use the setups in [15], where two-electron atoms generally have a spin-singlet ground state g and a long-lived spin triplet excited state e with opposite polarizabilities at some "anti-magic" wavelength, experiencing potentials with opposite signs and therefore aligning in a staggered manner. After loading, the resonant LG lasers then drive tunnelings between staggered states along a ring as $g \to e \to g \to e \to ....$ In this case, considering two inner states in g and e also generates the SU(2) field as shown in Fig. 1(e).

$SU(N)$ Gauge Field: In lattice Abelian gauge theories, the gauge transformation is defined as an U(1) transformation of the field operators if $O_i^0 \to O_i = e^{iX_i} O_i^0$ and the phase $\phi_{i,j}^0$ acquired in tunneling $e^{i\phi_{i,j}^0} \left(O_i^0\right)^\dagger O_j^0$ in the Hamiltonian is modified to $\phi_{i,j} = \phi_{i,j}^0 + X_i - X_j$. Under such gauge fields, the unitary transformation describing a particle hopping around a LG driving laser is given by the cumulative phase $\phi = \phi_{1,2} + \phi_{2,3} + \phi_{3,4} + \ldots \phi_{N_{\rm L}-1,N_{\rm L}} + \phi_{N_{\rm L},1}$, or the Wilson loop $W = e^{i\phi_{1,2}} e^{i\phi_{2,3}} e^{i\phi_{3,4}} \cdots e^{i\phi_{N_{\rm L}-1,N_{\rm L}}} e^{i\phi_{N_{\rm L},1}}$ where $N_{\rm L}$ is the number of lattice sites. This cumulative phase is related to the magnetic flux through the loop via the AB effect. When the center of the Raman laser is addressed to the middle of a plaquette or the center of the ring, numerical simulations for square- and ring-shaped lattices show that a non-uniform flux with accumulated phase π is generated for $l = 1$, in the form of an effective solenoid. The flux of the solenoid is entirely located within the plaquette or ring. We further note that even if the center of the laser is slightly shifted from that of the lattice, it will not affect the results in the thermodynamic limit, although some small fluctuations may appear around the solenoid. The phase generated in this manner corresponds to a vector potential of the form $\overrightarrow{A}_{\rm A} = (A_{{\rm A},x}, A_{{\rm A},y}, 0)$. With the lattice sites represented by (m, n) and lattice constant a, the vector potential can be written as

$$\overrightarrow{A}_{\rm A} \simeq \frac{\hbar c}{ea} (-1)^{m+n} \left(\varphi_{m,n}^{(x)}, \varphi_{m,n}^{(y)}, 0\right) \qquad (1)$$

in units of $\frac{\hbar c}{ea}$ according to the standard lattice gauge theory [24], where c is the light speed and e is an effective charge. Eq. (1) defines the mean Berry connection [11]. $\varphi_{m,n}^{(x)} = \int w_2^* (\overrightarrow{r} - \overrightarrow{r}_{m+1,n})\, \varphi(x,y)\, w_1 (\overrightarrow{r} - \overrightarrow{r}_{m,n})\, d^2\overrightarrow{r}$ and $\varphi_{m,n}^{(y)} = \int w_2^* (\overrightarrow{r} - \overrightarrow{r}_{m,n+1})\, \varphi(x,y)\, w_1 (\overrightarrow{r} - \overrightarrow{r}_{m,n})\, d^2\overrightarrow{r}$ with $\varphi(x,y)$ representing the phase of the Raman LG beam in the point (x,y).

When extending the $SU(1)$ transformation to $SU(N)$ by considering N inner states, the operator transformation becomes $O_i^0 \to O_i = T_i O_i^0$ with T_i a $N \times N$ matrix, and the Wilson loop W giving the state transformation as $|\psi\rangle \to W|\psi\rangle$ becomes $W = W_{1,2} + W_{2,3} + W_{3,4} + \ldots + W_{N_{\rm L}-1,N_{\rm L}} + W_{N_{\rm L},1}$ with $W_{i,j} = T_i^\dagger W_{i,j}^0 T_j$. When the loop operator is reduced to a global phase $W = e^{i\theta} I$ with I the $N \times N$ unit matrix, or equivalently the magnitude of Wilson loop is N, the system reduces to an Abelian system with N independent evolution equations for the N "flavor" components. For generating SU(2) fields, as for the example shown in Fig. 1(e), two degeneracies within the Zeeman manifolds should be considered. For example, for ^{40}K atoms, $m_F = \frac{9}{2}, \frac{7}{2}$ in $F = \frac{9}{2}$ and $m_F = \frac{7}{2}, \frac{5}{2}$ in $F = \frac{7}{2}$ represent two "colors" of the gauge field, and which become split when a moderate magnetic field is applied. Here we use a left-circularly polarized LG mode with $p = 0$, $l = 1$, and a superposition of two right-circularly polarized LG modes with $p = 0$, $l = 0$ and $p = 1$, $l = 0$ together to drive the spin-flipping transitions. We choose the beam width as $w/\sqrt{2} = N_{\rm L} a/(2\sqrt{2})$ for $l = 0$ laser and $w = N_{\rm L} a/2$ for $l = 1$ laser, such that the amplitudes $f_0(r) = \sqrt{\frac{1}{2}} e^{\frac{1}{2}(\frac{2r}{w})^2}$ and $f_1(r) = (\frac{\sqrt{2}r}{w})$ of lasers with angular momentums $l = 0$, 1 are approximately equal, which gives a unitary hopping matrix and generate a non-Abelian SU(2) field. The corresponding vector potential $\overrightarrow{A}_{\rm NA} = (A_{{\rm NA},x}, A_{{\rm NA},y}, 0)$ is given by

$$\begin{aligned} \overrightarrow{A}_{\rm NA} \simeq\ & \frac{1}{2}\overrightarrow{A}_{\rm A} + \frac{\pi}{2}\frac{\hbar c}{ea}\Big(\cos\frac{\varphi_{m,n}^{(x)}}{2}\sigma_x + \sin\frac{\varphi_{m,n}^{(x)}}{2}\sigma_y - 1, \\ & \cos\frac{\varphi_{m,n}^{(y)}}{2}\sigma_x + \sin\frac{\varphi_{m,n}^{(y)}}{2}\sigma_y - 1, 0\Big). \end{aligned} \qquad (2)$$

The unitary tunneling operators are $U(m, n \to m+1, n) = U_x(n)$, $U(m+1, n \to m, n) = U_x^\dagger(n)$, $U(m, n \to m, n+1) = U_y(m)$ and

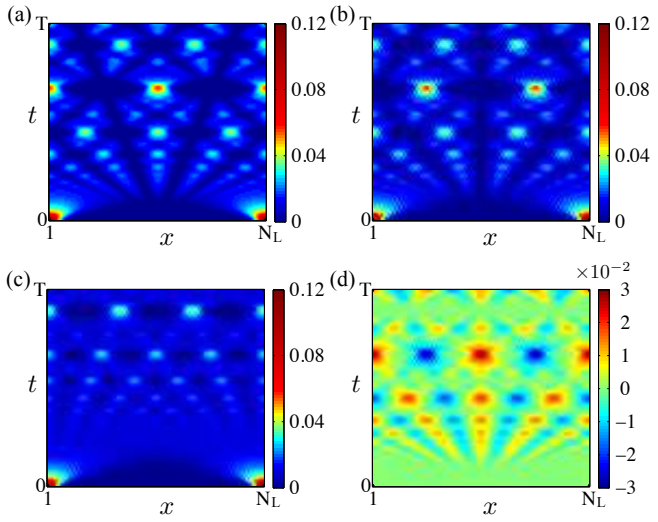

FIG. 2: The time evolution of particle distributions for particles hopping around a loop formed by LG beams in a ring with $N_{\mathrm{L}} = 100$ sites under a zero gauge field (a), an Abelian U(1) field (b), or a non-Abelian SU(2) field ((c) and (d)). The particle densities are represented by the percentages of particle numbers to the total number of the initially prepared Bose-Einstein condensate. At time $t = 0$, the particles are prepared around the site $x = 1$. During the time period from $t = 0$ to $t = T = 600J^{-1}$, the fringe patterns around the opposite site $x = N_{\mathrm{L}}/2$ become completely different for the three field cases ($B = 0$, U(1) and SU(2)). Around this site, there is always a constructive interference for the zero field case in (a) and a destructive interference in (b). In contrast, for the non-Abelian case, the charge wave density, the sum of the two effective spins, has no unique behavior as shown in (c), and the spin wave density, as a difference of the two effective spins, exhibits two kinds of spin waves as shown in (d), where the red-color (blue-color) spin wave has a constructive (destructive) interference around the site $x = N_{\mathrm{L}}/2$ and a destructive (constructive) interference around the nearest neighboring area.

$U(m, n+1 \to m, n) = U_y^\dagger(m)$, where $U_x = \exp(-ieaA_{\mathrm{NA},x}/\hbar c)$ and $U_y = \exp(-ieaA_{\mathrm{NA},y}/\hbar c)$. The appearance of the phase factor in $U_x(n)\,U_y(m+1)\,U_x^\dagger(n+1)\,U_y^\dagger(m)$ can be understood in terms of the AB phase accumulated by the particles when they travel along a closed contour [11].

Dynamical evolution and AB effect: We load a Bose-Einstein condensate (BEC) around one site, away from the center of LG-laser, and allow the system to evolve under different gauge fields. We then measure the fringe patterns with time. For a 1D ring-shaped optical lattice as illustrated in Fig. 1(b), numerical simulations for spatial distributions of particle numbers are plotted in Fig. 2, where the particle numbers are shown as a percentage to the total number in the initially prepared BEC. We have chosen the lattice site number as $N_{\mathrm{L}} = 100$ and the time period T as 600 in unit of J^{-1},where the typical hopping $J \simeq 0.05E_R$ with E_R the recoil energy. Distinctly different interference pattens can be seen for particles experiencing a zero magnetic field as shown in (a), an Abelian U(1) gauge field as shown in (b), and a non-Abelian SU(2) gauge field as shown in (c)-(d). The reason for the two subfigures in the SU(2) case is that two effective spins are involved in the SU(2) field. We plot an effective charge wave density (the sum of densities of the two effective spins) in (c) and an effective spin wave density (the difference of densities of the two effective spins) in (d), respectively.

At time $t = 0$, a BEC is prepared around site $x = 1 \equiv N_{\mathrm{L}} + 1$, as shown in Fig. 2. After the initial state is prepared, we turn on the LG beams. For the zero-magnetic field case in Fig. 2(a), we turn on a laser with $l = 0$, and for the U(1) Abelian field case in (b), we turn on a $l = 1$ laser as illustrated in Fig. 1(d), and for the non-Abelian SU(2) field case in (c) and (d), we turn on two orthogonally polarized $l = 0$ and $l = 1$ lasers as illustrated in Fig. 1 (e). After a certain time, we see that the particle number distributions around the site $x = N_{\mathrm{L}}/2$, directly opposite to the initially occupied site, are different in the three cases [see Fig. 2 (a)-(c)]. Note that a destructive interference is always seen in Fig. 2 (b) at site $N_{\mathrm{L}}/2$. The spin wave density in (d) can be regarded as a difference of two effective spin densities: one colored red and the other blue in Fig. 2 (d). At site $N_{\mathrm{L}}/2$, the constructive interference is always due to one type (red). This result can also be explained as a superposition of two effective spin waves under a zero gauge field due to the $l = 0$ laser and a finite gauge field due to the $l = 1$ laser. The red-color spin wave therefore represents the spin wave sensitive to the zero magnetic field and the blue-color spin wave represents the other spin wave sensitive to the non-zero magnetic field.

Our key result for the ring geometry is a clear demonstration of the AB effect. In the presence of an Abelian synthetic gauge field, the AB phase always induces destructive interference at site $N_{\mathrm{L}}/2$. Absence of any population at site $N_{\mathrm{L}}/2$ at any time is therefore a clear signature of the Abelian AB effect. Furthermore, we demonstrate the effects of the non-Abelian gauge field in terms of the spin density waves.

For the 2D square lattice case as illustrated in Fig. 1(a) and 1(c), we can also prepare the initial state by loading a BEC around one plaquette. For the U(1) Abelian field case as shown in Fig. 3(b), we turn on a $l = 1$ laser as illustrated in Fig. 1(d), and for the non-Abelian SU(2) field case as shown in Fig. 3 (c)-(d), we turn on two orthogonally polarized $l = 0$ and $l = 1$ lasers as illustrated in Fig. 1(e). Numerical simulations with time show that the angular momentum imparted by the LG beams results in a circular distributions of atoms. The particle number distribution at the opposite side of the circle from the initially prepared site again shows clear destructive interference in the case of the Abelian gauge field - the signature of the AB effect. As a concrete ex-

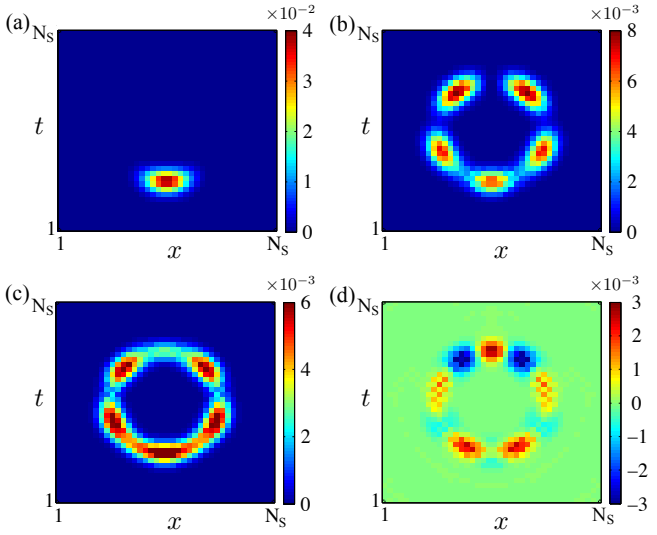

FIG. 3: The time evolution of particle distributions for particles hopping around a loop formed by LG beams in a 2D square lattice with 40×40 sites. At time $t = 0$ as shown in (a), the particles are distributed around one site. The screenshots at time $t = 2000J^{-1}$ are given for the system under an Abelian U(1) (b) or a non-Abelian SU(2) ((c) and (d)) gauge field. The particle densities are represented by the percentages of particle numbers to the total number of the initially prepared Bose-Einstein condensate. While a destructive interference always occurs around the opposite site in the Abelian field case (b), a non-vanishing charge wave density occurs everywhere in (c) and two kinds of spin waves appear in (d) as red- and blue-colored spin waves, where the red-color (blue-color) spin wave has a constructive (destructive) interference at the opposite side and a destructive (constructive) interference at its two neighboring area.

ample, screenshots at time $t = 4000J^{-1}$ are given in Fig. 3 (b)-(d). The effect is similar to the ring geometry case.

In summary, we have presented a method for generating Abelian and non-Abelian synthetic gauge fields with cold atoms. As an example of the use of this method, we demonstrate an interferometric scheme to observe directly the AB effect. We also illustrate interference patterns for charge and spin density waves corresponding to the non-Abelian AB analogue. These effects are robust against decoherence as they are topological in origin. Consequently, they could in principle be harnessed for quantum information processing [25–27]. We have demonstrated a method for generating U(1) and SU(2) gauge fields, this technique in principle can be generalized to SU(N).

We acknowledge support from the National Research Foundation & Ministry of Education, Singapore.

[1] Y. Aharonov and D. Bohm, Phys. Rev. **115**, 485 (1959).
[2] M.V. Berry, Proc. R. Soc. Lond. A, **392**, 45 (1984).
[3] R.G. Chambers, Phys. Rev. Lett. **5**, 3 (1960); G. Möllenstedt and W. Bayh, Naturwissenschaften **49**, 81 (1962); W. Bayh, Z. Phys. **169**, 492 (1962); V.G. Schaal, C. Jönsson, and E.F. Krimmel, Optik **24**, 529 (1966).
[4] A. Tonomura, *et al.* Phys. Rev. Lett. **56**, 792-795 (1986).
[5] A. Caprez, B. Barwick, and H. Batelaan. Phys. Rev. Lett. **99**, 210401 (2007).
[6] R.A. Webb, S. Washburn, C.P. Umbach, and R.B. Laibowitz, Phys. Rev. Lett. **54**, 2696 (1985); S. Washburn and R.A. Webb, Rep. Prog. Phys. **55**, 1311 (1992); G. Timp, *et al.*, Phys. Rev. Lett. **58**, 2814 (1987); A. Fuhrer, *et al.*, Nature **413**, 822-825 (2001); Microelectron. Eng. **63**, 47 (2002).
[7] S. Russo, *et al.* Phys. Rev. B **77**, 085413 (2008); J. Schelter, P. Recher and B. Trauzettel. Solid State Comm. **152**, 1411 (2012), and references therein.
[8] M. Bayer,*et al.* Phys. Rev. Lett. **90**, 186801 (2003).
[9] E. Ribeiro, A.O. Govorov, W. Carvalho, Jr., and G. Medeiros-Ribeiro. Phys. Rev. Lett. **92**, 126402 (2004); Igor L. Kuskovsky, *et al.* Phys. Rev. B **76**, 035342 (2007).
[10] A. Bachtold, *et al.* Nature **397**, 673-675 (1999); S. Zaric, *et al.* Science **304**, 1129-1131 (2004).
[11] J. Dalibard, F. Gerbier, G. Juzeliūnas, and P. Öhberg. Rev. Mod. Phys. **83**, 1523 (2011).
[12] M. Lewenstein, *et al.*, Adv. Phys. **56**, 243-379 (2007); T.-L. Ho, Phys. Rev. Lett. **87**, 060403 (2001).
[13] G. Juzeliūnas, P. Öhberg, J. Ruseckas, and A. Klein, Phys. Rev. A **71**, 053614 (2005); J. Ruseckas, G. Juzelūnas, P. Öhberg, and M. Fleischhauer, Phys. Rev. Lett. **95**, 010404 (2005); G. Juzelūnas and P. Öhberg, Phys. Rev. Lett. **93**, 033602 (2004).
[14] Y.-J. Lin, *et al.*, Phys. Rev. Lett. **102**, 130401 (2009); Y.-J. Lin, R.L. Compton, K. Jiménez-García, J.V. Porto and I.B. Spielman, Nature **462**, 628-632 (2009).
[15] K. Osterloh, M. Baig, L. Santos, P. Zoller, and M. Lewenstein, Phys. Rev. Lett. **95**, 010403 (2005); D. Jaksch and P. Zoller, New J. Phys. **5**, 56 (2003); F. Gerbier and J. Dalibard, New J. Phys. **12**, 033007 (2010); N. Goldman, A. Kubasiak, P. Gaspard, and M. Lewenstein, Phys. Rev. A **79**, 023624 (2009).
[16] A. Klein and D. Jaksch, Europhysics Lett. **85**, 13001 (2009).
[17] P.J. Wang, *et al.* Phys. Rev. Lett. **109**, 095301 (2012); L.W. Cheuk, *et al.* Phys. Rev. Lett. **109**, 095302 (2012).
[18] M. Aidelsburger, *et al.* Phys. Rev. Lett. **107**, 255301 (2011).
[19] M. Z. Hasan and C. L. Kane, Rev. Mod. Phys. **82**, 3045 (2010).
[20] X-L Qi and S.C. Zhang, Rev. Mod. Phys. **83**, 1057 (2011).
[21] A. Kitaev and C. Laumann, arXiv:0904.2771 (2009).
[22] L. Amico, A. Osterloh and F. Cataliotti, Phys. Rev. Lett. **95**, 063201 (2005).
[23] A. Bermudez, *et al.*, Phys. Rev. Lett. **105**, 190404 (2010); Z. Lan, N. Goldman, A. Bermudez, W. Lu and P. Ohberg, Phys. Rev. B **84**, 165115 (2011); Leonardo Mazza, *et al.*, New J. Phys. **14**,s 015007 (2012).
[24] I. Montvay and G. Münster, *Quantum Fields on a Lattice* (Cambridge University Press, Cambridge, 1994); H.J. Rothe, *Lattice Gauge Theories* (World Scientific, Singapore, 1998).
[25] P.J. Leek *et al.*, Science **318**, 1889 (2007).

[26] J.A. Jones, V. Vedral, A. Ekert, and G. Castagnoli, Nature **403**, 869 (2000).

[27] G. Falci *et al.*, Nature **407**, 355 (2000).